BJR

Received: 19 March 2013 | Revised: 20 June 2013 | Accepted: 27 June 2013

doi: 10.1259/bjr.20130163

Cite this article as:
Mori S, Inaniwa T, Furukawa T, Zenklusen S, Shirai T, Noda K. Effects of a difference in respiratory cycle between treatment planning and irradiation for phase-controlled rescanning and carbon pencil beam scanning. Br J Radiol 2013;86:20130163.

FULL PAPER

Effects of a difference in respiratory cycle between treatment planning and irradiation for phase-controlled rescanning and carbon pencil beam scanning

S MORI, PhD, T INANIWA, PhD, T FURUKAWA, PhD, S ZENKLUSEN, PhD, T SHIRAI, PhD and K NODA, PhD

Medical Physics Research Group, Research Center for Charged Particle Therapy, National Institute of Radiological Sciences, Chiba, Japan

Address correspondence to: Dr Shinichiro Mori
E-mail: *shinshin@nirs.go.jp*

Objective: To evaluate the impact of variation in respiratory cycle between treatment planning and irradiation for pencil beam scanning and phase-controlled rescanning (PCR) on the resulting dose distribution, we conducted a simulation study based on four-dimensional CT (4DCT) data for lung cancer patients.
Methods: 4DCT data were acquired for seven patients with lung tumours. Treatment planning was designed to ensure the delivery of 95% of the prescribed dose to the clinical target volume in respective phases of the 4DCT by taking account of intrafractional beam range variations. Carbon ion pencil beam scanning dose distributions were calculated for various respiratory cycles that differed from the reference respiration (=4.4 s) but which stayed regular during irradiation. The number of rescannings was changed to 1, 4 or 8 times. PCR was correlated with the gating window in treatment planning to calculate the beam weighting map.
Results: 8×PCR improved dose conformation to the target for all irradiation respiratory cycles. Minimum dose (D_{min}) and lowest dose encompassing 95% of the target (D_{95}) values with 4×PCR were decreased from 94.1% and 98.1% to 88.4% and 93.5% with an altered irradiation respiratory cycle of 2.4 s. However, these values were improved with 8×PCR to over 94.9% for D_{min} and 98.6% for D_{95} for respective irradiation respiratory cycles.
Conclusion: Pencil beam scanning treatment with eight or more PCRs consistently improved dose conformation for moving lung targets even when different respiratory cycles were used for treatment planning and irradiation.
Advances in knowledge: Scanning treatment with eight or more rescannings consistently improved dose homogeneity to a moving target even though respiratory cycles varied during treatment.

Charged particle beams provide superior dose conformation to photon beams, and more than 28 particle treatment centres have now been established worldwide. Since 1994, our centre at Heavy Ion Medical Accelerator in Chiba, Japan, has treated over 7000 cancer patients using carbon ion passive beams [1–3]. In 2011, we constructed a new treatment facility for carbon ion pencil beam scanning (C-PBS) as an extension of the existing treatment facility and successfully completed the first clinical trials for the head and pelvic regions with non-respiratory-gated irradiation at the end of 2011 [4,5]. We are now preparing to start the next series of clinical trials for the thoracic and abdominal regions.

Organ motion is a major challenge in radiotherapy and can both degrade dose conformation within a tumour and cause excessive dosages to normal tissues. Organ motion as a result of respiratory motion is now well understood, and several problems have been recognised. First, if respiratory-induced tumour motion is not considered in treatment planning, the treatment beam will not irradiate the tumour owing to its movement in and out of the beam field with respiration. Second, because the stopping position of a charged particle beam is strongly dependent on the radiological pathlength from the patient surface, replacing dense tissue with a low-density material such as lung causes a significant change in radiological pathlength, resulting in the perturbation of beam stopping position from that originally planned. Although passive scattering beam irradiation delivers homogeneous three-dimensional (3D) dose distributions that cover the whole tumour region at any time, C-PBS delivers respective beam spots as a function of time. Scanning irradiation is accordingly less robust against organ motion than passive beam delivery owing to interplay effects that cause hot and/or cold spots within the target owing to the inconsistency between beam motion and target motion [6]. Proposed remedies for this problem include respiratory gating, tracking [7] and rescanning [8] strategies, of which gating and rescanning are preferable from a practical point of view. For C-PBS at our institute, the beam spots are sorted and delivered in layers of spots of the same range/energy,

called isoenergy layers, on the basis that the speed of scanning in the lateral direction is much higher than the variation of range. Our approach to the moving tumour problem is a combination of layered rescanning correlated with the gating window, which we term "respiratory phase-controlled-layered rescanning (PCR)". We measured dose distribution with PCR under a motion scenario using Gafchromic™ films (Ashland Inc., Covington, KY) in which four or more PCRs achieved dose differences of less than 2% of that with the static case [9]. Measurement showed higher target dose homogeneity for PCR than was obtained without correlated rescanning. A similar approach has been proposed for proton beam therapy [10].

However, several problems remain to be solved before clinical treatment of tumours in the thoracic and abdominal regions with C-PBS can be started. Most treatment planning processes assume that patient respiratory cycle and pattern remain reproducible throughout the course of treatment and do not address interfractional variation. The respiratory pattern is variable, however, and this may lead to rescanning of an isoenergy layer to fail to finish within a gate window, resulting in inconsistencies between treatment planning and treatment beam delivery. This remains a fundamental challenge to PCR in thoracic and abdominal treatment.

Here, we evaluated the impact of respiratory cycle variation between treatment planning and treatment beam irradiation on dose distribution for four-dimensional (4D) C-PBS of a lung tumour using a 4DCT scan-based dose calculation.

METHODS AND MATERIALS

Rescanning methods

Our centre provides integrated hybrid C-PBS [11]. This scanning method uses a mini ridge filter (to create a mini spread-out Bragg peak), a range shifter and 11 synchrotron energies. The range shifter and energy changes can be adjusted in 3- and 30-mm range steps, respectively. In the present study, we set control times for the range shifter and synchrotron energy changes to 420 and 150 ms, respectively [12,13]. Hybrid scanning provides a superior lateral dose fall-off and a higher relative biological effectiveness than can be obtained with the range shifter only because less range shifter material is needed [11]. The beam characteristics are comparable with those with the sole use of the synchrotron for energy variation but require less commissioning work.

PCR performs the rescanning of all spots of a layer within the gating window such that the rescanning of the layer is completed at the end of the gating window. After finishing one layer, the energy/range is changed and the next layer is irradiated. This process is repeated until all spots of the entire set of layers are delivered. To achieve this strategy, the dose rate for respective isoenergy layers is calculated from the gating window time and is set by the radiation system before the delivery of each layer. Therefore, once the treatment is started, the irradiation pattern (beam spot, dose rate, etc.) cannot be changed even though the patient respiratory pattern may have changed. Figure 1a shows the scan pattern with a perfectly regular respiratory signal for a gated PCR with two rescannings. All spots in the mth and all spots in the $m+1$th isoenergy layers were rescanned twice within their respective gates; namely, once each in the first and subsequent gating window. Beam weights in the gating window within the same isoenergy layer were the same but differed from those of the respective isoenergy layers. However, if the irradiation respiratory cycle changes from that in treatment planning, not all beam spots will be completed at the end of the gating window, and PCR will not be achieved. Remaining spots will be delivered at the start of the next gate and will then be followed by energy variation during the gate window, which will further prolong treatment and desynchronize PCR, as illustrated in Figure 1b. In that case, beam spots in the mth isoenergy layer were irradiated twice, each for a shorter duration than in the first gating window, and several spots in the $m+1$th isoenergy layer were irradiated in the same gating window. When the irradiation respiratory cycle was shorter than the planning respiratory cycle, in contrast, beam spots in the mth isoenergy layer irradiation were completed before the end of the gating window and start of irradiation of the next isoenergy layer.

PATIENTS

Seven of our lung cancer patients were randomly selected (Table 1) and asked for their consent to participate in this study. The study protocol was approved by the Institutional Review Board of our institute. 4DCT was carriedout with a fast-rotating area detector CT [14] under free-breathing conditions, with patient respiration monitored using a respiratory sensing system consisting of a position-sensitive detector and an infrared-emitting light marker (PSM15010; Toyonaka Kenkyujo, Osaka, Japan). CT voxel size was 512×512×128 [0.78 mm (anteroposterior) × 0.78 mm (left–right) × 1.0 mm (superoinferior)]. Motion parameters, including respirator cycles and Euclidian distance of the 3D centre of mass (3D-COM) of the gross tumour volume (GTV), are summarised in Table 1.

Treatment planning

Target definition

A single respiratory cycle was subdivided into 10 equal phases (T00: peak inhalation, T50: peak exhalation). The GTV was delineated on the 4DCT data at T50. All GTV contours at other respiratory phases for the patient were then automatically calculated by B-spline-based deformable image registration (DIR) [15,16]. Clinical target volume (CTV) included the GTV plus a 10-mm margin. The beam weighting map was designed to ensure uniform dose distribution to CTVs in respective phases. The internal target volume (ITV) included the target-encompassing volume within the gating window; however, the International Commission on Radiation Units and Measurements Report 62 describes the "geometrical" rather than the "radiological path-length" concept for ITV creation [17]. Maximum intensity volume (MIV) and average intensity projection (AIP), approaches which have been introduced in passive particle beam irradiation [18,19], were successfully used to deliver the treatment beam to a moving target using a treatment planning system that was commercially available at that time. Because these methods may result in expansion of the smeared beam field and density regions, however, and consequently cause overdosage to the normal tissue regions, they have not been completely optimised to allow for intrafractional range variations [20]. Further, given that intrafractional dose degradation with passive beam occurs as a blurring effect, whereas scanning irradiation suffers from

Figure 1. (a) Irradiation respiratory cycle (=T_1) is the same as that for the planning respiratory cycle. The gating window for treatment planning is from t_1 to t_3 and from t_4 to t_5. Two PCR layers are present. (b) The irradiation respiratory cycle (=T_2) is longer than that for the planning respiratory cycle (=T_1). The gating window for the irradiation is from t_1' to t_3' and from t_4' to t_7. PCR, phase-controlled rescanning.

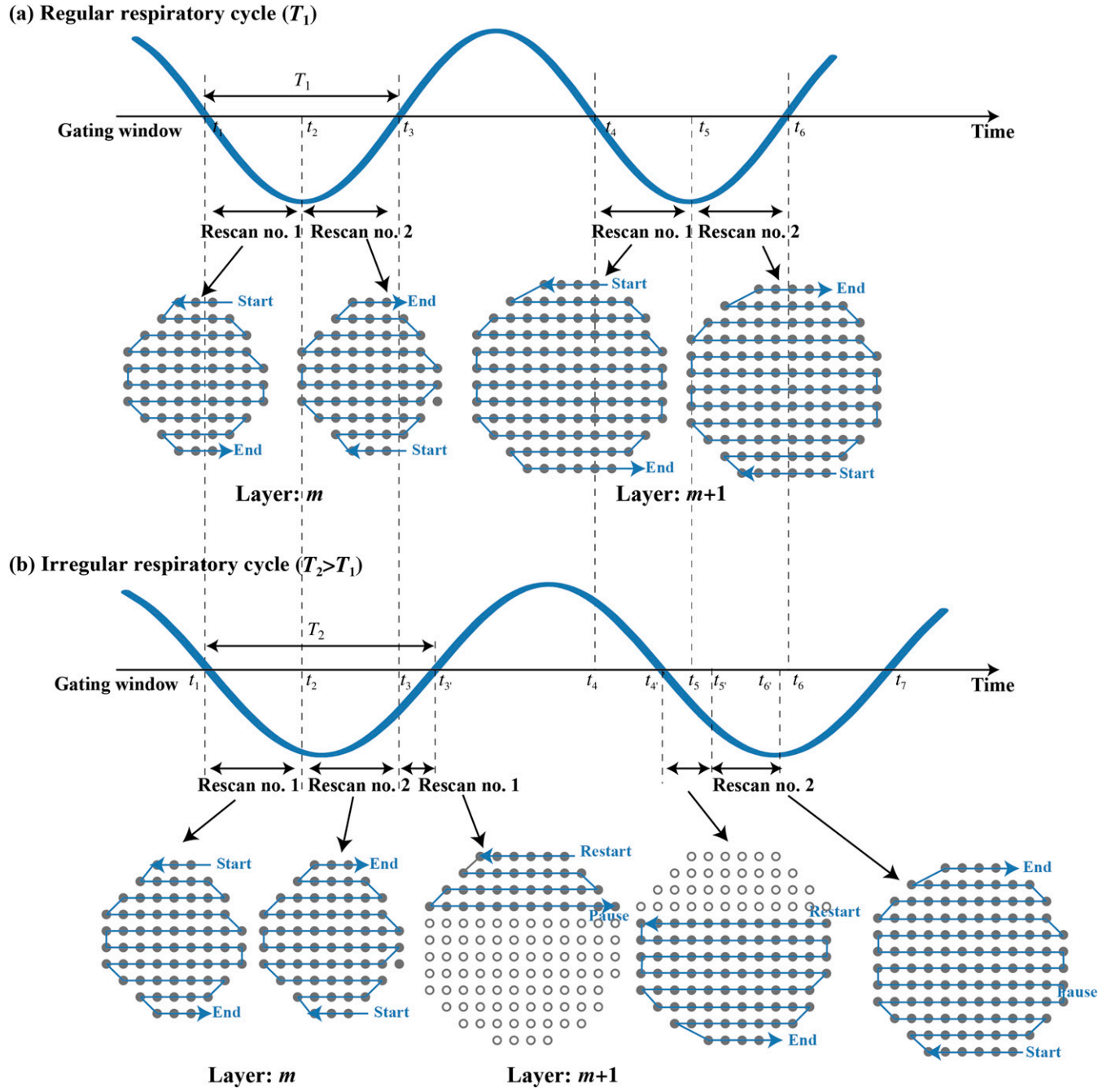

not only blurring but also the interplay effect, the inability of both MIV and AIP to completely compensate for intrafractional range variation renders them particularly unsuitable for particle beam therapy. To solve this problem, we defined the field-specific target volume (FTV), which is considered robust in 3D treatment planning and has been applied in 4D treatment planning using passive beam irradiation. First, beam ranges were calculated from the beam entrance of the patient surface to the distal and proximal edge of the CTV for the respective phases within the gating window. The FTV was then calculated by selecting the minimum and maximum beam ranges ray by ray. Since no setup margin was added to the FTV, planning target volume (PTV) was the same as the FTV.

DOSE CALCULATIONS

The dose distributions for C-PBS were calculated for a respiratory-ungated strategy. Simulated scanning speed in the superoinferior and left–right directions were 100 mm ms^{-1} and 50 mm ms^{-1},

Table 1. Respirator motion characteristics of patients

Patient number	Gender	Age (years)	T stage	Location		Pathology	Original respiratory cycle (s)	3D-COM (mm)
1	M	76.0	Meta	Right lower lobe	S6	Meta	3.8	5.5
2	M	75.0	T2N0M0	Right lower lobe	S10	SCC	3.1	12.4
3	M	64.0	T2N1M0	Left upper lobe	S4	SCC	4.4	4.9
4	F	65.0	Meta	Right lower lobe	S7	Meta	5.5	8.9
5	M	61.0	T1N0M0	Right lower lobe	S8	ADC	3.6	7.7
6	M	72.0	T2N0M0	Right lower lobe	S10	SCC	2.7	17.4
7	F	79.0	T1N0M0	Right lower lobe	S9	S9	2.8	5.0
Mean		70.3					3.7	8.8
SD		6.9					1.0	4.6

ADC, adenocarcinoma; 3D-COM, three-dimensional centre of mass; F, female; M, male; Meta, metastasis; SCC, squamous cell carcinoma; SD, standard deviation.

respectively. Measurements were performed to irradiate a 60-mm spherical water target with a nominal dose of 1 Gy and a carbon beam intensity of 1.5×10^8 pps (particle per second) within approximately 18 s [13]. Although this measurement used the range shifter scanning technique, the total treatment time was of a similar order. Beam spot positions and beam weights were optimised for the PTV. Spot spacing was 2.0 mm laterally and 3.0 mm in the beam direction, and lateral scatter (80–20%) was approximately 5 mm.

The prescribed dose of 52.8 GyE (3.3 GyE×16 fr) was administered to respective PTVs via four beam ports from the ipsilateral rather than the contralateral side of the tumour. The respiratory cycle during 4DCT acquisition was used to calculate the beam weighting map to respective phases (Figure 1a). To evaluate the impact of a difference in respiratory cycle between treatment planning and treatment beam delivery on dose distribution, we performed dose distribution for different respiratory cycles by applying the dose rate and scanning speed defined in the planning respiratory cycle (Figure 1b). Use of the respiratory cycle averaged over all seven patients of 3.7 s as a planning respiratory cycle would result in a small range of irradiation respiratory cycle variation (*e.g.* 1.7–6.7 s). It is well known that patient respiratory cycle can change during treatment; however, a cycle of 1.7 s is not suitable in clinical situations. We previously found that the mean respiratory cycle in 85 lung cancer patients treated with gating in our centre was 4.4 s and used this value in our present planning respiratory cycle. Given that respiratory cycle differs among patients, and that we were concerned here with the magnitude of the different respiratory cycle from the reference cycle rather than the original respiratory cycle in this study, we used cycles from 2.4 to 7.4 s in 1-s steps to calculate dose distribution (irradiation respiratory cycle). To maximally emphasise the difference in respiratory cycle between treatment planning and irradiation, we selected an irradiation respiratory cycle from 2.4 to 7.4 s for all irradiation times as a worst-case scenario. The number of rescannings was altered between single scanning (denoted as one rescan) and two, four and eight times rescanning on the basis of our previous study, which evaluated the impact of rescanning number on dose distribution using a numeric moving phantom. Results showed that dose homogeneity within the target was improved by increasing the number of rescannings and that four or more PCRs under the same respiratory cycle between treatment planning and irradiation were largely satisfactory [21].

To emphasise the impact of intrafractional motion on dose distribution, the gating window was defined as all respiratory phases. Dose distributions within the gating window were calculated using 4DCT data sets, and the accumulated dose was calculated by registering dose distribution at respective phases to that at the peak exhalation phase (T50) using the appropriate DIR. DIR accuracy was quantified by manual checking of feature points. The average over all patients for the whole thoracic region, area around the target region and ipsilateral lung was 1.1 mm (<1.7 mm), 0.8 mm (<1.5 mm) and 1.3 mm (<2.3 mm), respectively. All 4DCT data sets were transferred to a workstation and analysed using the Aqualyzer system, which calculates the 4D carbon ion beam dose distribution as a function of time [22]. Dose assessment metrics were evaluated in lowest dose encompassing 95% of the target (D_{95}), maximum dose (D_{max}), minimum dose (D_{min}) for CTV at the reference respiratory phase (T50) and homogeneity index (HI). HI is calculated as the standard deviation of the accumulated dose because even though it represents a single voxel, it could be affected by maximum dose.

RESULTS

Dose distributions for a four-field plan [all single field uniform dose (SFUD)] are shown in Figure 2. The magnitude of hot/cold

spots was reduced compared with a single beam angle. The prescribed dose was successfully given to the target by applying 4×PCR and 8×PCR (D_{95}: 98% and D_{min}: 95% of the prescribed dose), but dose differences were observed when altering the irradiation respiratory cycles of 2.4 s or 7.4 s. The magnitude of dose differences was smaller for a higher number of rescannings, such as 8×PCR. D_{95} values with 1×PCR, 4×PCR and 8×PCR were 96.2%, 98.1% and 98.1% for a planning cycle of 4.4 s, and 95.8%, 97.0% and 98.1% for an irradiation cycle of 2.4 s. For an irradiation cycle of T=7.4 s, D_{95} values for 1×PCR, 4×PCR and 8×PCR were 93.5%, 97.4% and 97.7%, respectively.

Results for a four-field plan (all SFUD) calculated for another example (Patient 4) are shown in Figure 3. Significant underdosage to the CTV was observed for the irradiation respiratory cycle of 2.4 s without rescanning (1×PCR) and to a lesser extent for 4×PCR (white arrows in Figure 3a,b). D_{max}/D_{min} values for 1×PCR and 4×PCR were 113%/89% and 107%/93%, respectively. By contrast, the accumulated dose with 8×PCR showed substantially improved dose conformation, and dose differences were very small (Figure 3c).

In Figure 4, we summarise the averaged dose assessment metrics of all single fields over all patients as a function of respiratory cycle and number of rescannings; in other words, for a four-field plan, we calculated D_{95} for each field individually. Figure 4a,b shows that averaged D_{95} and D_{min} values for 4×PCR were decreased to 93.5% and 82.9%, respectively, at an irradiation respiratory cycle of 2.4 s. By contrast, values with 8×PCR were improved to over 97.6% and 93.6%, respectively. D_{max} and D_{min} mean values with 4×PCR were almost the same as those with 8×PCR (D_{max}/D_{min}=109%/94%), whereas D_{min} with 4×PCR at an irradiation respiratory cycle of 2.4 s was decreased to 88.4% (Figure 4b). D_{max}/D_{min} value variations were minimised with 8×PCR. HI values showed a similar tendency to the previous two metrics, with HI mean value with 8×PCR also remaining constant (1.9–2.4%) (Figure 4c).

Figure 5 summarises the dose assessment metrics for the four-field plans averaged over all patients, *i.e.* by first calculating the accumulated dose over the four fields and then calculating D_{95}, etc. Results showed a similar tendency to those of the single beam fields, but magnitudes were improved by averaging the four beam angles (Figure 5). D_{95} and D_{min} values with 8×PCR were >99.0% and 96.1%, respectively, whereas D_{max} and HI values were <104.3% and 1.5%, respectively.

DISCUSSION

In this study, we evaluated the impact of variation in respiratory cycle between the treatment planning and irradiation stages on 4D dose distribution using lung 4DCT data sets. Our results showed that eight PCRs improved dose conformity better than a single or four rescannings, with less dependency on respiratory cycle variation. Since we used the area detector 4DCT, a prototype of a commercially available 320 multislice CT that acquires an approximately 13-cm scan range in a single rotation [14], our 4DCT images do not exhibit the banding artefacts frequently seen in conventional 4DCT. Our results therefore represent a more accurate method for 4D dose calculation.

Figure 2. Four-field carbon ion beam dose distribution for (a) 1×PCR, (b) 4×PCR and (c) 8×PCR (Patient 3). Yellow and green lines show the CTV and PTV, respectively. Light blue, orange, pink and red lines show the 105%, 100%, 95% and 90% doses, respectively. Planning respiratory cycle was 4.4 s. Dose differences for the irradiation respiratory cycle of 4.4 s were zero, as expected. CTV, clinical target volume; PCR, phase-controlled rescanning; PTV, planning target volume.

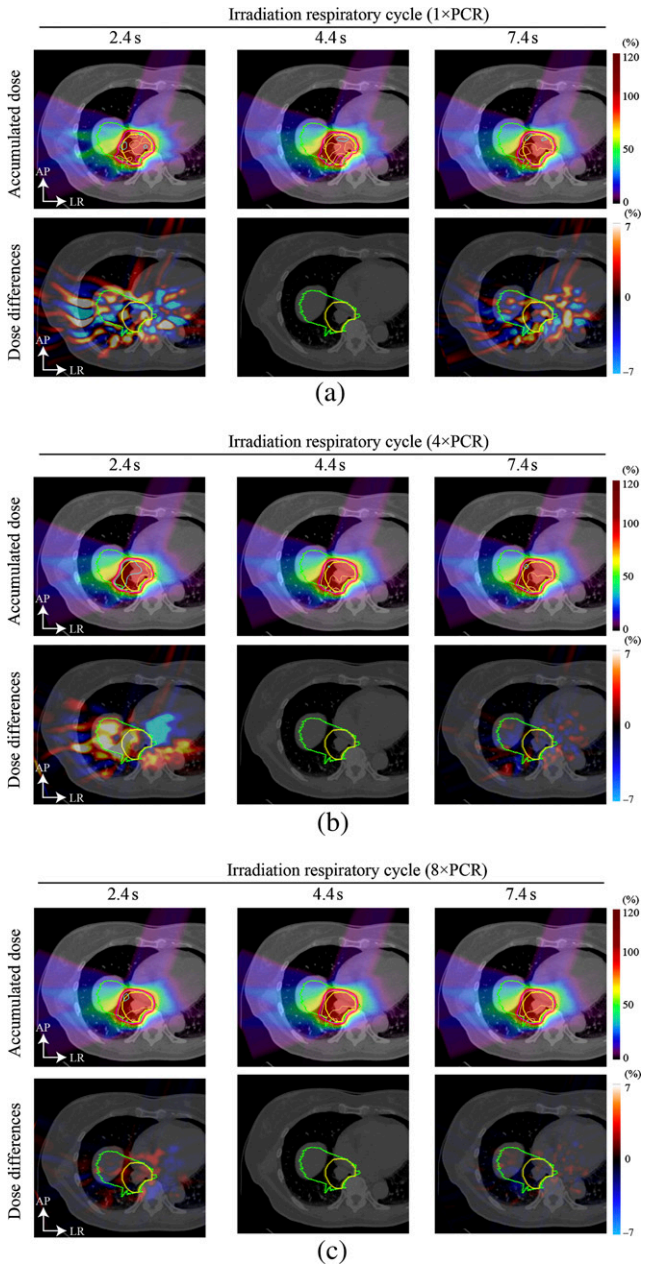

Dose variation

Two cases showed in this study were smallest and average COM, albeit that, the dose differences for 1×PCR and 4×PCR when the respiratory cycle was changed from the original one. A case with a large COM might emphasise the dose differences. Intrafractional motion causes dose degradation in two major ways. First, replacement of the solid tumour density by the lower density of the lung following positional change as a function of

Figure 3. Four-field carbon ion beam dose distribution with four different beam angles for (a) 1×PCR, (b) 4×PCR and (c) 8×PCR (Patient 4). Beam angles were 20°, 70°, 110° and 160°. Yellow and green lines show the CTV and PTV, respectively. Light blue, orange, pink and red lines show the 105%, 100%, 95% and 90% doses, respectively. The planning respiratory cycle was 4.4 s. Dose differences for the irradiation respiratory cycle of 4.4 s were zero, as expected. CTV, clinical target volume; PCR, phase-controlled rescanning; PTV, planning target volume.

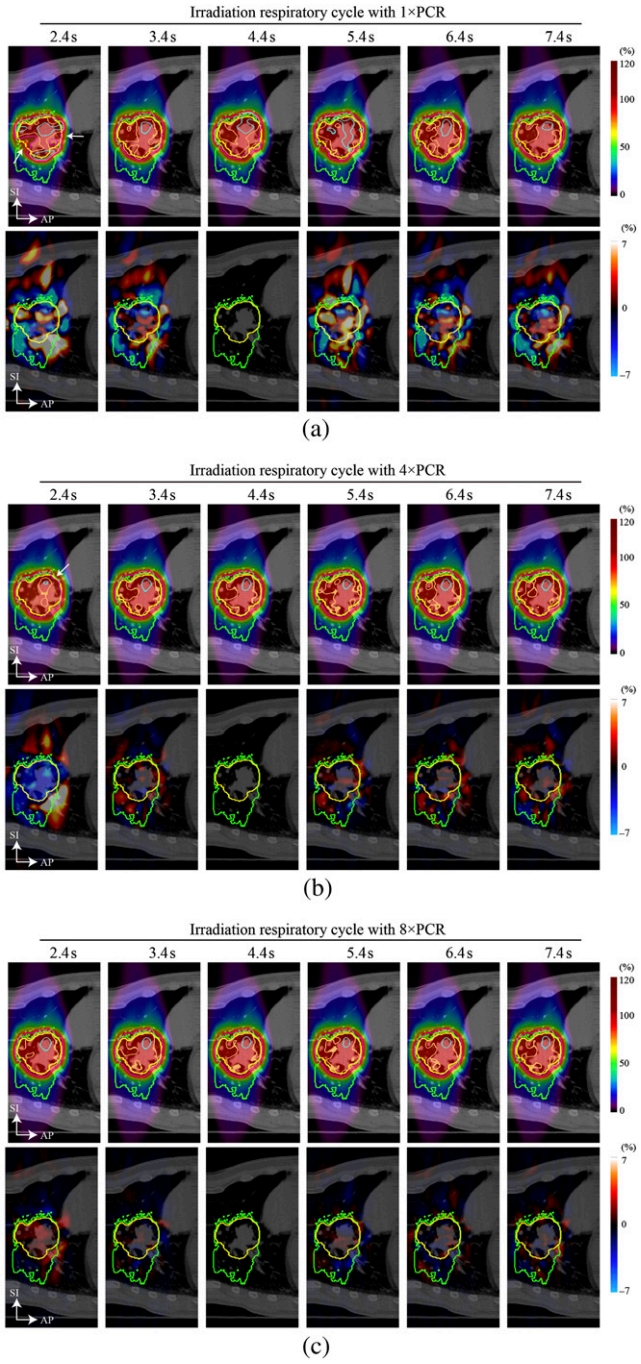

respiratory phase causes beam overshoot and undershoot. In the irradiation respiratory cycle of 4.4 s with 8×PCR, *e.g.* beam overshoot was observed in both the superior and inferior directions (upper row in Figure 2c). Overshoot occurred when the target moved in the inferior direction, whereas undershoot occurred in the reverse situation. This is because a large number of rescannings increased scanning speed and decreased dose rate, with the result that the beam could be configured close to a broad shape. This situation is similar to layer-stacking rather than passive scattering beam irradiation [23]. Dose conformation with 8×PCR showed no particular degradation, even though the irradiation respiratory cycle was changed from the planning respiratory cycle.

By contrast, dose conformation to the moving target was degraded with 1×PCR even though the respiratory cycle was the reference phase (=4.4 s) and treatment was conducted around peak exhalation. Scan speed for 1×PCR is eight times slower than that for 8×PCR while the dose rate is eight times higher. Moreover, the beam shape is far from a broad beam shape. These conditions might emphasise interplay effects between beam delivery and organ motion. Our results showed that the magnitude of beam overshoot and undershoot differed in the superior and inferior sides.

Dose conformation with 4×PCR was improved over that with 1×PCR in respective irradiation respiratory cycles, whereas scanning speed and dose rate were less advantageous than with 8×PCR. The magnitude of beam overshoot in the superior and inferior sides favoured 8×PCR. Moreover, when the irradiation respiratory cycle was changed, dose conformation with 4×PCR was less robust than that with 8×PCR.

We evaluated dose distribution with respiratory cycles that differed from an artificial reference cycle rather than from a patient-specific original cycle. Given that the magnitude of the difference in respiratory cycles might affect dose variation, a similar tendency to those seen in this study might also be seen for dose distributions calculated by changing the respiratory cycle from the original cycle.

Practical approaches

We clarified that multiple PCR improved dose conformity to the moving organ even though the respiratory cycle changed during treatment. A treatment protocol that integrates this into treatment should be designed before the start of PCR treatment for the thoracic and abdominal regions.

We previously evaluated respiratory cycles for a total 331 patients selected from our hospital under thoracic and abdominal conditions, including 85 with lung cancer, and obtained data for 523 cycles throughout the treatment course. The respiratory cycle averaged over all lung patients was 3.6 s (SD, 0.9 s; range, 2.1–7.1 s). From these results, 8×PCR would appear to provide better dose conformity (D_{95} >95% in respective irradiation respiratory cycles) at a clinically acceptable level in lung scanning treatment particularly since we observed difficulties for a lower number of rescannings for small respiratory cycles.

With regard to the planning respiratory cycle, this was defined by averaging respective respiratory cycles acquired during 4DCT. Most treatment centres perform 4DCT using multislice CT, which requires several tens of seconds to acquire the whole scanning region needed for treatment planning. The planning respiratory cycle was therefore calculated by averaging multiple

Figure 4. Results for dose metrics averaged over all single beam angles in all patients for (a) D_{95}, (b) maximum dose (D_{max})/minimum dose (D_{min}) and (c) homogeneity index (HI). PCR, phase-controlled rescanning.

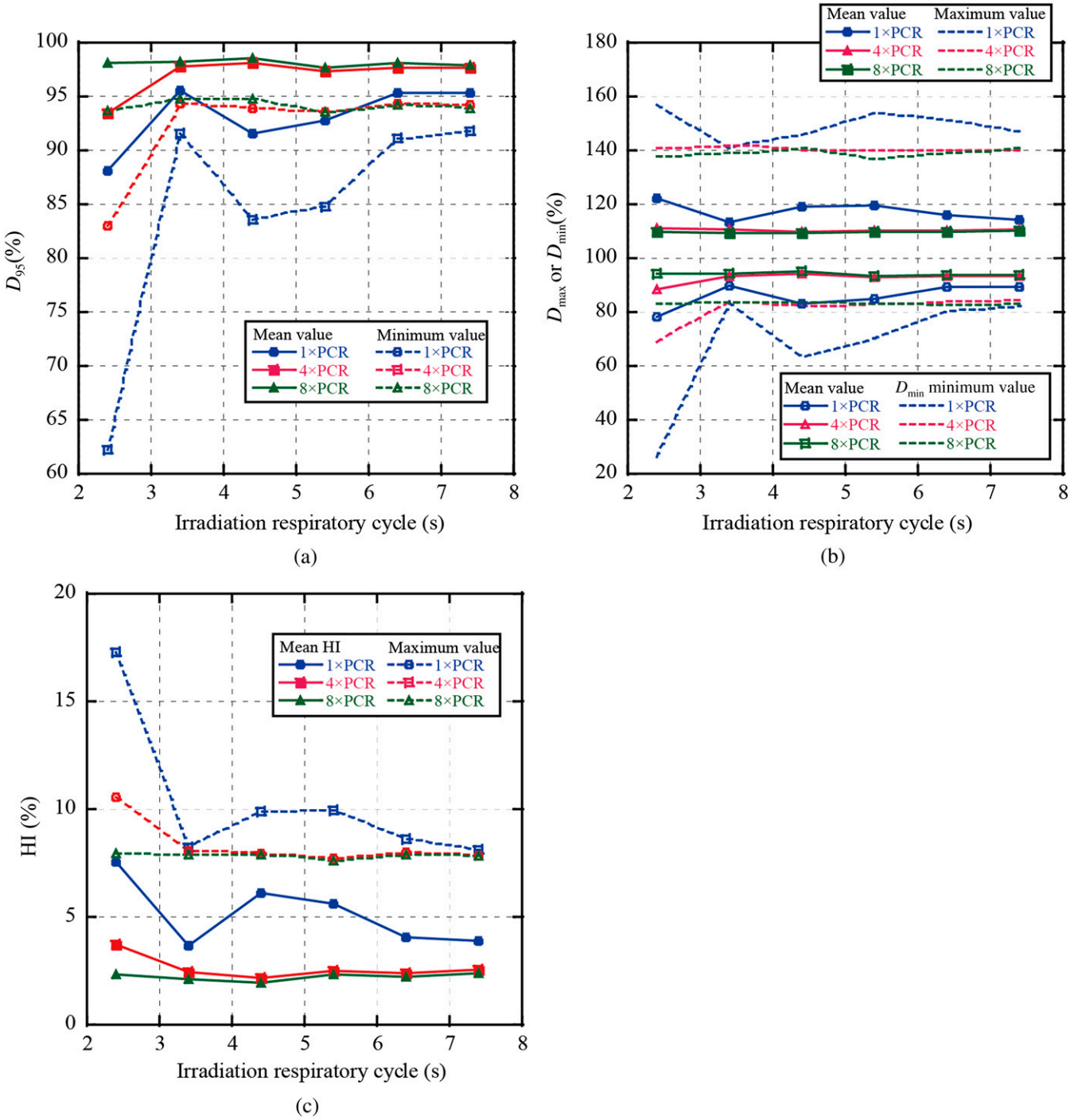

respiratory cycles, which thereby took account of respiratory pattern variations. Although area detector CT acquires only a single or a few respiratory cycles in 4D mode, it is better to acquire several respiratory cycles before or after 4DCT and calculate the planning respiratory cycle using these data.

Study limitations

Several limitations of this study warrant mention. First, respiratory characteristics of patients are not strictly regular, and generally vary in amplitude and cycle from one cycle to the next [24,25]. Since this study focused on dose variation owing to respiratory cycle differences between treatment planning and irradiation stages, we assumed that patient respiratory cycle was reproducible throughout the course of treatment. The accumulated dose in scanning irradiation is the summed pencil beam dose distribution at respective positions in 3D space. On this basis, changes in target position when the planned beam spots are irradiated in different parts

Figure 5. Results for dose metrics averaged over all patients with four-field plans for (a) D_{95}, (b) maximum dose (D_{max})/minimum dose (D_{min}) and (c) homogeneity index (HI). PCR, layered phase-correlated rescan.

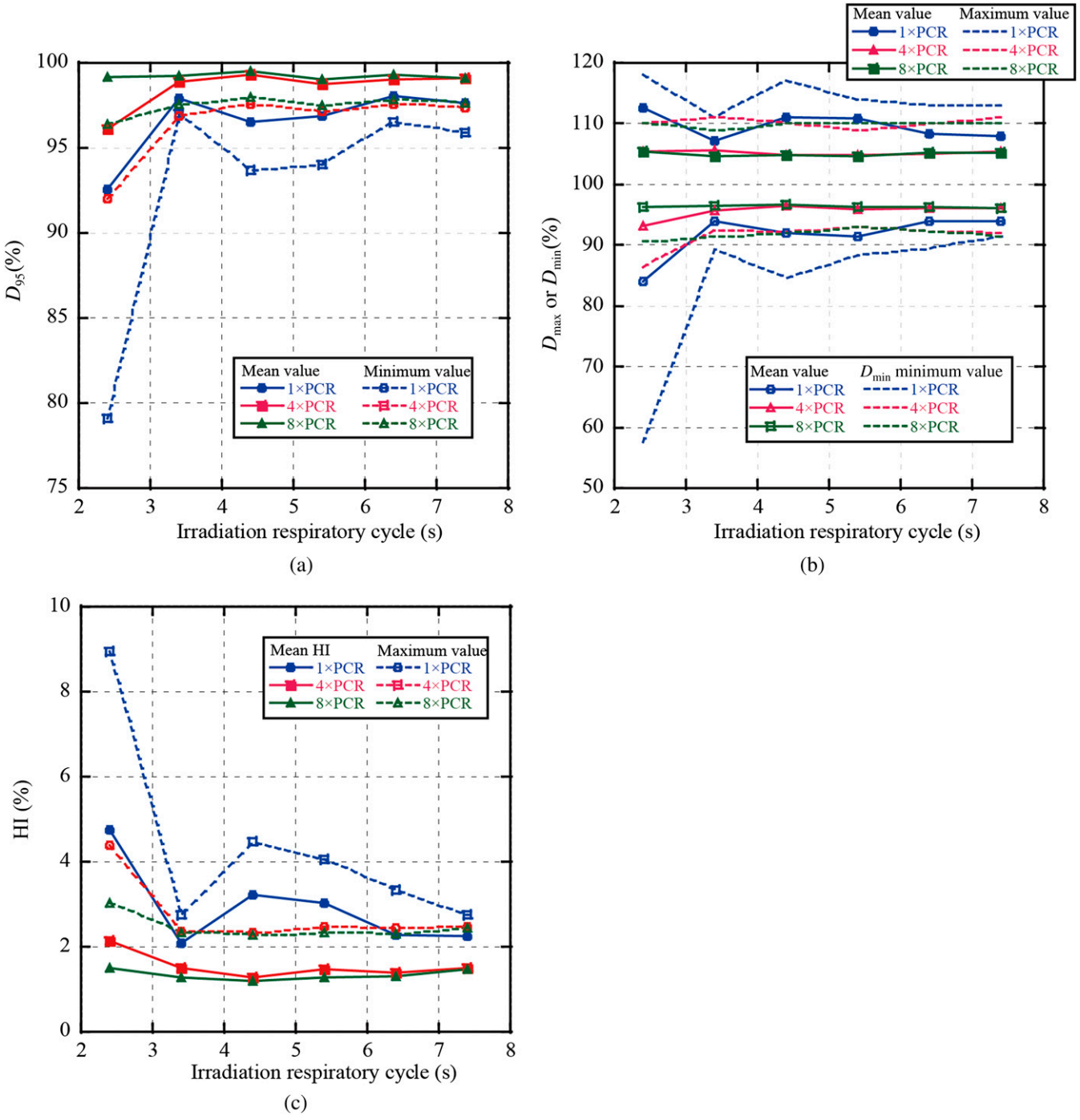

of the respiratory phase might result in the degradation of dose conformity. The magnitude of dose variation owing to this factor might not be improved by applying the respiratory gating strategy.

Second, the patient respiratory cycle does not remain the same during treatment in clinical settings. This study was not conducted under clinical conditions but did apply various irradiation respiratory cycles during treatment to reflect conditions under a worst-case scenario. The impact of dose variation under clinical conditions might accordingly be smaller than in this study.

CONCLUSION

We quantified 4D dose distribution between treatment planning and irradiation with consideration of DIR for respiratory cycle

variation. Current treatment planning uses a single respiratory cycle only because the inclusion of respiratory patterns during irradiation cannot be accounted for. The relationship between planning and irradiation respiratory cycles is particularly important for PCR, which delivers pencil beam irradiation to respective spots correlated with the patient's respiratory cycle. From our study, scanning treatment with eight or more rescannings consistently improved dose homogeneity to the moving target even though respiratory cycle during treatment varied. We consider that these results will aid in improving treatment accuracy in scanning beam therapy.

ACKNOWLEDGMENTS

We wish to express our appreciation to Drs Masayuki Baba, Naoyoshi Yamamoto and Mio Nakajima for their acquisition of 4DCT data.

REFERENCES

1. Okada T, Kamada T, Tsuji H, Mizoe JE, Baba M, Kato S, et al. Carbon ion radiotherapy: clinical experiences at National Institute of Radiological Science (NIRS). J Radiat Res 2010;51:355–64.
2. Eiichi T. Carbon ion radiotherapy at NIRS-HIMAC. Nucl Phys A 2010;834:730c–5c.
3. Tsujii H, Kamada T. A review of update clinical results of carbon ion radiotherapy. Jpn J Clin Oncol 2012;42:670–85. doi: 10.1093/jjco/hys104.
4. Mori S, Shibayama K, Tanimoto K, Kumagai M, Matsuzaki Y, Furukawa A, et al. First clinical experience in carbon ion scanning beam therapy: retrospective analysis of patient positional accuracy. J Radiat Res 2012; 53:760–8. doi: 10.1093/jrr/rrs017.
5. Mori S, Shirai T, Takei Y, Furukawa T, Inaniwa T, Matsuzaki Y, et al. Patient handling system for carbon ion beam scanning therapy. J Appl Clin Med Phys.2012; 13:226–40.
6. Bert C, Grözinger SO, Rietzel E. Quantification of interplay effects of scanned particle beams and moving targets. Phys Med Biol 2008;53:2253–65. doi: 10.1088/0031-9155/53/9/003.
7. Grozinger SO, Bert C, Haberer T, Kraft G, Rietzel E. Motion compensation with a scanned ion beam: a technical feasibility study. Radiat Oncol 2008;3:34. doi: 10.1186/1748-717X-3-34.
8. Phillips MH, Pedroni E, Blattmann H, Boehringer T, Coray A, Scheib S. Effects of respiratory motion on dose uniformity with a charged particle scanning method. Phys Med Biol 1992;37:223–34.
9. Furukawa T, Inaniwa T, Sato S, Shirai T, Mori S, Takeshita E, et al. Moving target irradiation with fast rescanning and gating in particle therapy. Med Phys 2010;37:4874–9.
10. Seco J, Robertson D, Trofimov A, Paganetti H. Breathing interplay effects during proton beam scanning: simulation and statistical analysis. Phys Med Biol 2009;54:N283–94. doi: 10.1088/0031-9155/54/14/N01.
11. Inaniwa T, Furukawa T, Kanematsu N, Mori S, Mizushima K, Sato S, et al. Evaluation of hybrid depth scanning for carbon-ion radiotherapy. Med Phys 2012;39:2820–5. doi: 10.1118/1.4705357.
12. Iwata Y, Kadowaki T, Uchiyama H, Fujimoto T, Takada E, Shirai T, et al. Multiple-energy operation with extended flattops at HIMAC. Nucl Inst Methods Phys Res A 2010;624:33–8.
13. Furukawa T, Inaniwa T, Sato S, Shirai T, Takei Y, Takeshita E, et al. Performance of the NIRS fast scanning system for heavy-ion radiotherapy. Med Phys 2010;37:5672–82.
14. Mori S, Endo M, Tsunoo T, Kandatsu S, Tanada S, Aradate H, et al. Physical performance evaluation of a 256-slice CT-scanner for four-dimensional imaging. Med Phys 2004;31:1348–56.
15. Wu Z, Rietzel E, Boldea V, Sarrut D, Sharp GC. Evaluation of deformable registration of patient lung 4DCT with subanatomical region segmentations. Med Phys 2008;35:775–81.
16. Sharp GC, Kandasamy N, Singh H, Folkert M. GPU-based streaming architectures for fast cone-beam CT image reconstruction and demons deformable registration. Phys Med Biol 2007;52:5771–83. doi: 10.1088/0031-9155/52/19/003.
17. International Commission on Radiation Units and Measurements—62. Prescribing, recording and reporting photon beam therapy (supplement to ICRU Report 50). Bethesda, MD: International Commission on radiation Units and Measurements; 1999.
18. Kang Y, Zhang X, Chang JY, Wang H, Wei X, Liao Z, et al. 4D Proton treatment planning strategy for mobile lung tumors. Int J Radiat Oncol Biol Phys 2007;67:906–14. doi: 10.1016/j.ijrobp.2006.10.045.
19. Rietzel E, Liu AK, Doppke KP, Wolfgang JA, Chen AB, Chen GT, et al. Design of 4D treatment planning target volumes. Int J Radiat Oncol Biol Phys 2006;66:287–95. doi: 10.1016/j.ijrobp.2006.05.024.
20. Mori S, Wu Z, Folkert MR, Kumagai M, Dobashi S, Sugane T, et al. Practical approaches to four-dimensional heavy-charged-particle lung therapy. Radiol Phys Technol 2010;3:23–33. doi: 10.1007/s12194-009-0072-3.
21. Mori S, Furukawa T, Inaniwa T, Zenklusen S, Nakao M, Shirai T, et al. Systematic evaluation of four-dimensional hybrid depth scanning for carbon-ion lung therapy. Med Phys 2013;40:031720. doi: 10.1118/1.4792295.
22. Mori S, Chen GT. Quantification and visualization of charged particle range variations. Int J Radiat Oncol Biol Phys 2008;72:268–77. doi: 10.1016/j.ijrobp.2008.05.011.
23. Kanematsu N, Endo M, Futami Y, Kanai T, Asakura H, Oka H, et al. Treatment planning for the layer-stacking irradiation system for three-dimensional conformal heavy-ion radiotherapy. Med Phys 2002;29:2823–9.
24. Chi Y, Liang J, Yan D. A material sensitivity study on the accuracy of deformable organ registration using linear biomechanical models. Med Phys 2006;33:421–33.
25. Benchetrit G. Breathing pattern in humans: diversity and individuality. Respir Physiol 2000;122:123–9.